For submission to *Nature Photonics*

Supplementary Information

for

Probing Perovskite Carrier Dynamics under Sunlight

Bo-Han Li [a, d, †], Huang Li [a, c, †], Zhipeng Xuan [b, †], Wen Zeng [a, d], Jia-Cheng Wang [a, d], Chuanyao Zhou [a], Xingan Wang [c], Jingquan Zhang [b, *], Zefeng Ren [a, *] and Xueming Yang [a, e]

a) State Key Laboratory of Molecular Reaction Dynamics and Dynamics Research Center for Energy and Environmental Materials, Dalian Institute of Chemical Physics, Chinese Academy of Sciences, Dalian 116023, China

b) Institute of Solar Energy Materials and Devices, College of Materials Science and Engineering, Sichuan University, No. 24 South Section 1, Yihuan Road, Chengdu 610065, China

c) Department of Chemical Physics, University of Science and Technology of China, Hefei, 230026, China.

d) University of Chinese Academy of Science, 19 A Yuquan Road, Beijing, 100049, P. R. China

e) Department of Chemistry, Southern University of Science and Technology, 1088 Xueyuan Road, Guangdong, Shenzhen, 518055, China

† These authors contributed equally to this work.

* Authors to whom correspondence should be addressed.

Email addresses: zhangjq@scu.edu.cn; zfren@dicp.ac.cn

1. Sample preparation

Materials: PbI_2 (> 99.99%, TCI), $CH(NH_2)_2I$ (FAI, >99.99%, Greatcell), CsI (>99.9%, Xi'an PLT), $PbCl_2$ (>99.9%, Xi'an PLT), N,N-Dimethylformamide (DMF, anhydrous, >99.8%, Sigma-Aldrich), Dimethyl sulfoxide (DMSO, anhydrous, >99.9%, Sigma-Aldrich), Chlorobenzene (CB, anhydrous, > 99.5%, Sigma-Aldrich).

Perovskite films were prepared using the one-step method. The Corning glass substrates with the dimension of 1.5×1.5 cm^2 were soaked in detergent for 2 hours, followed by ultrasonic cleaning for 15 min in absolute ethanol, deionized water and absolute ethanol sequentially, and then blow dried with N_2 gas for later use. The perovskite precursor was obtained by dissolving 0.9 mmol formamidinium iodide (FAI), 0.1 mmol CsI and 1 mmol PbI_2 into 1 mL DMF/DMSO (9:1 volume ratio) and stirring sufficiently. The substrates were pre-treated with ultraviolet-ozone for 15 min and the perovskite layer was prepared in a glovebox filled with N_2 by augmented spin coating method. The mentioned perovskite precursor was spin-coated at 1000 rmp for 10 s and then rotated at 6000 rpm for 15 s where 100 μL CB antisolvent was dripped on perovskite films before ending the program. Subsequently, the wet perovskite film was annealed at 100 ℃ for 10 min.

2. Sample characterization

X-ray diffraction (XRD) spectra were recorded by an X-ray diffractometer (LabX XRD-6100 SHIMADZU). The photoluminescence (PL) spectra were measured by the Edinburgh Instruments FLS 980 fluorescence spectrometer. The UV-vis absorption spectra were performed by Lambda 950 UV/Vis spectrophotometer (PeikinElmer Inc). The surface morphology was measured by the Zeiss field emission SEM (Hitachi S-4800) equipped with EDS.

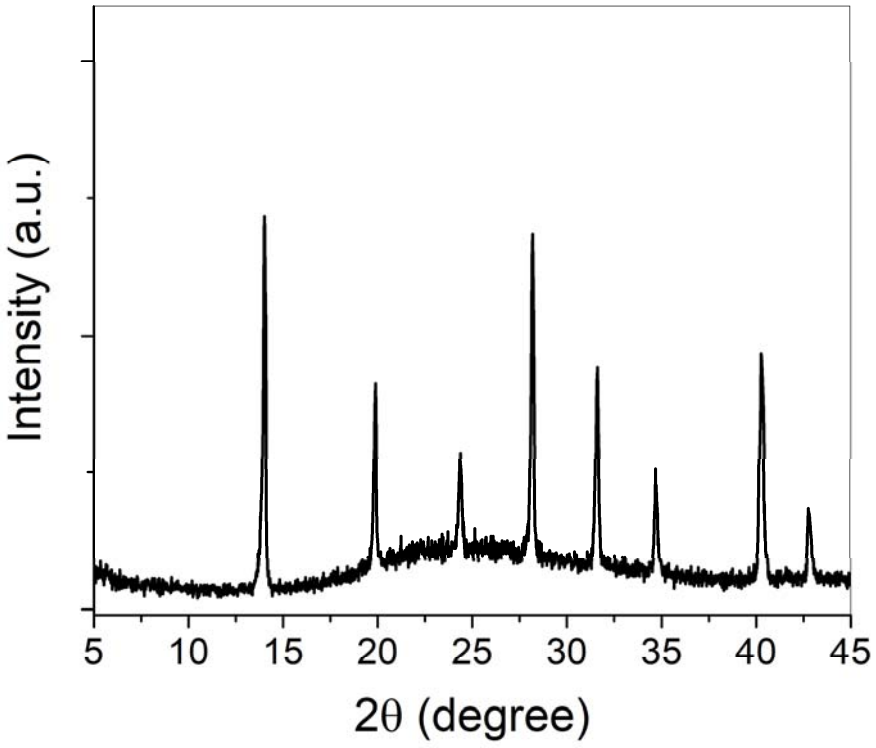

Figure S1. XRD spectra of $Cs_{0.1}FA_{0.9}PbI_3$ thin film.

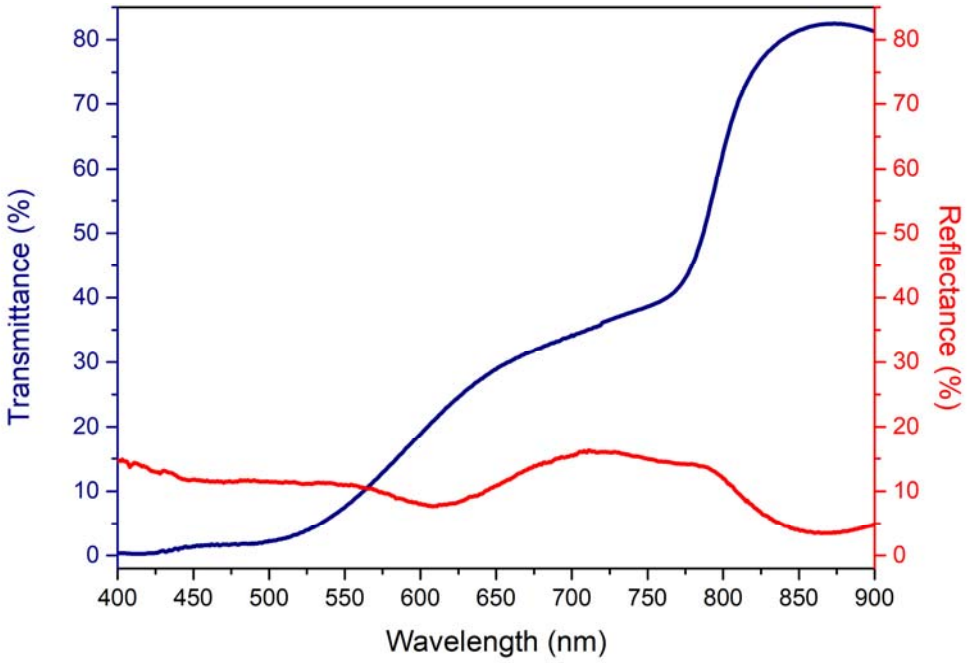

Figure S2. Reflection and transmission spectra of a 253-nm thick $Cs_{0.1}FA_{0.9}PbI_3$ thin film.

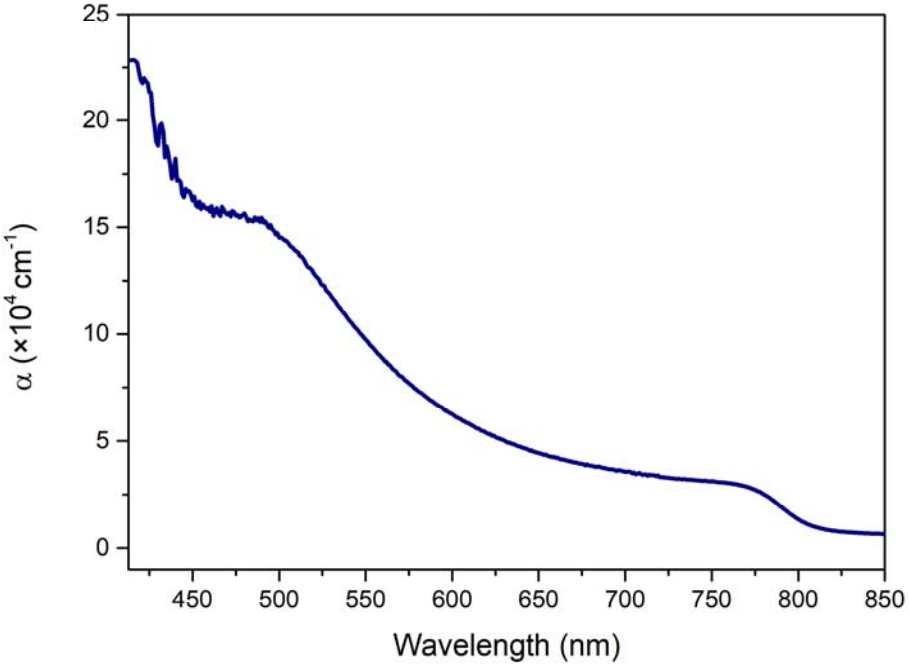

Figure S3. Absorption coefficient of $Cs_{0.1}FA_{0.9}PbI_3$ thin film as a function of wavelength.

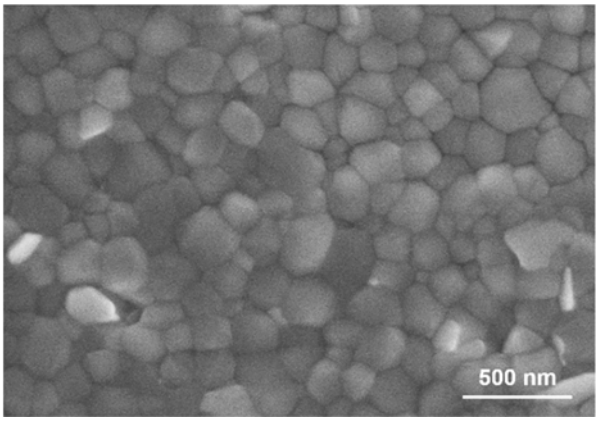

Figure S4. SEM image of $Cs_{0.1}FA_{0.9}PbI_3$ thin film.

3. Transient absorption measurements

The transient absorption measurement was based on a fiber laser (1030 nm, pulse duration ~230 fs, 1 MHz repetition rate) and recently developed pump-probe transient absorption spectrometer.[1] The repetition rate of the fundamental beam output was divided down to 200 kHz as micro-pulses, and then modulated at 1 kHz as macro-pulse.

The number of micro-pulses in a macro-pulse was selected based on the signal-to-noise ratio. The output was split into two beams. One beam was to generate second harmonics (515 nm) or sent to an optical parametric amplifier (CHOPAS-G, BC-Light) to generate the pump pulse, and its intensity was tuned by the combination of a half waveplate and a polarization beamsplitter (PBS). The pump light was modulated at 500 Hz of macro-pulses by a chopper. The other 1030 nm was focused into a sapphire crystal to generate supercontinuum. Then it was split into two beams by using an achromatic waveplate and a PBS. One enters a monochromator and was collected by a photodiode (PD) as the reference light, and the other was focused and then passed through the sample as the probe light, collimated and dispersed with a monochromator and finally probed by the other PD, with integrating 3 nm bandwidth FWHM of the probe light. Both PDs were connected to a balanced transimpedance amplifier and then a lock-in amplifier. The pump-probe delay can be up to ~4 ns tuned by a delay line. The pump and probe were focused and overlapped onto the sample. The pump size is dia. 3 mm for 515 nm, and dia. 3.5 mm for 690 nm, and the probe size is about dia. 0.6 mm.

4. Sample stability

To keep the sample stable during experiment, it was sealed in a sample cell in the glove box, which schematically shows in S5. The atmosphere in the sample cell was the same as in the glove box. Both sides of the sample cell were fused silica, which was suit for TA measurements. This protects perovskites from water and oxygen and keeps stable for more than one week. The stability of $Cs_{0.1}FA_{0.9}PbI_3$ thin films in the sample cell was checked by measuring the TA curves of the fresh sample and the sample kept in the cell for one week. Figure S5 shows both TA curves are identical, implying that the sample in the cell was stable.

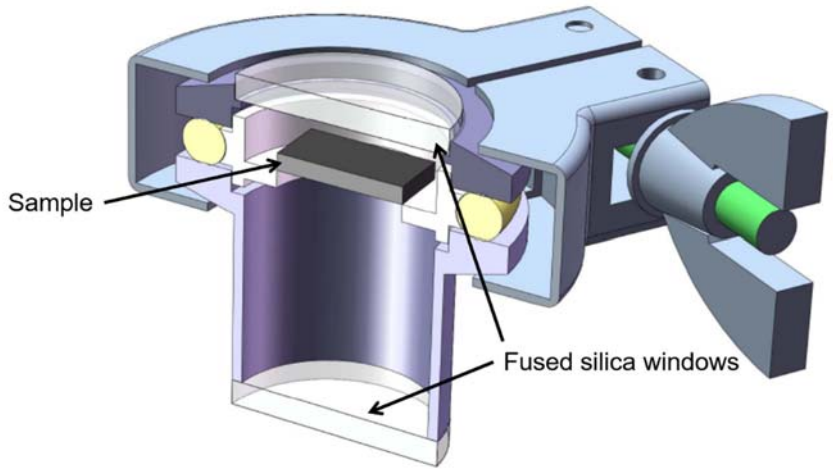

Figure S5. Schematic of sample cell sealed by KF flange.

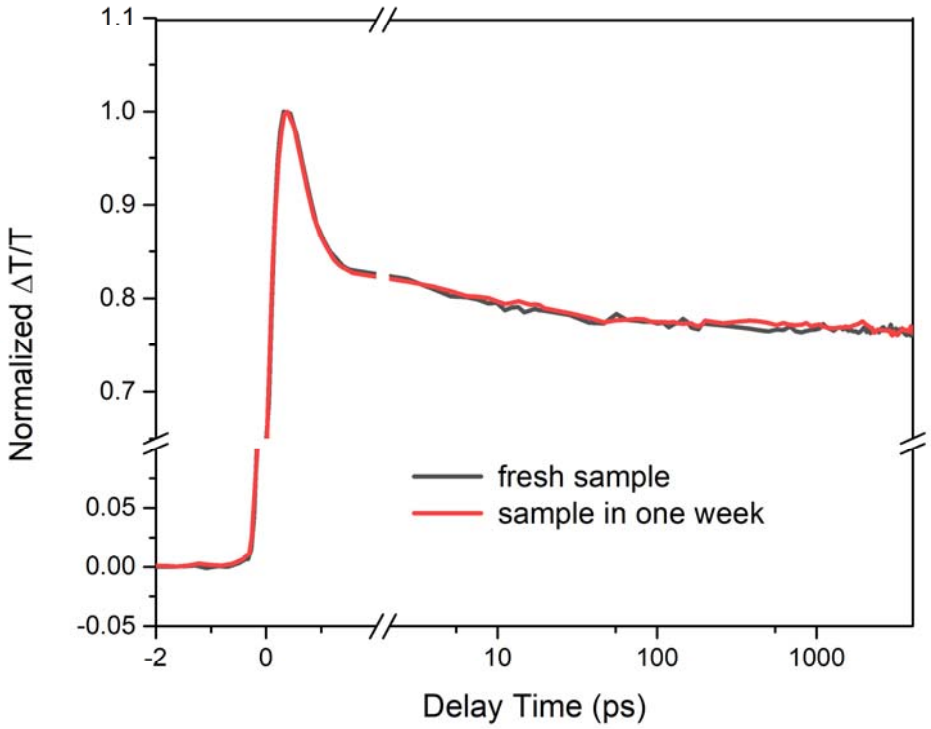

Figure S6. Stability test of thin film. TA dynamics measurements of $Cs_{0.1}FA_{0.9}PbI_3$ thin films. Comparison of TA dynamics curves of the fresh sample (dark line) and the sample kept in the cell (red line) for one week. The pump wavelength is 515 nm with 3 nJ per pulse and the probe is 790 nm.

5. Initial carrier density estimation

The photogenerated carrier density *n* is estimated as following expression

$$n = \frac{P_{in}(1-R)(1-1/e)}{h\nu \cdot A \cdot d} \quad \text{(S1)}$$

where P_{in} is the pump pulse energy, R is the reflectivity of the perovskite film at the excitation wavelength, $h\nu$ is the photon energy of the pump, A is the area of the pump beam, and d is the penetration depth of the pump in the sample, which is equal to 1/α. For $Cs_{0.1}FA_{0.9}PbI_3$ thin film, R is about 11.3% and 15.0% at 515 and 690 nm, respectively. The fused silica window transmission of the sample cell is about 93%. The pump laser diameter is 3 mm at 515 nm and 3.5 mm at 690 nm. The penetration depth is 74 nm at 515 nm and 270 nm at 690 nm. Hence, the photogenerated carrier density is corresponding to about 2.6×10^{15} cm^{-3} with pump energy 1 nJ per pulse at 515 nm, and 6.7×10^{14} cm^{-3} with pump energy 1 nJ per pulse at 690 nm.

6. Pump intensity-dependent TA dynamics at the pump wavelength of 690 nm

Figure S7 shows the TA spectra with pump wavelength of 690 nm and 50 nJ per pulse. Pump intensity-dependent TA dynamics was measured to obtain the linear response range, as shown in Figure S8. It shows the pump energy at about 10 nJ reaches the linear response range.

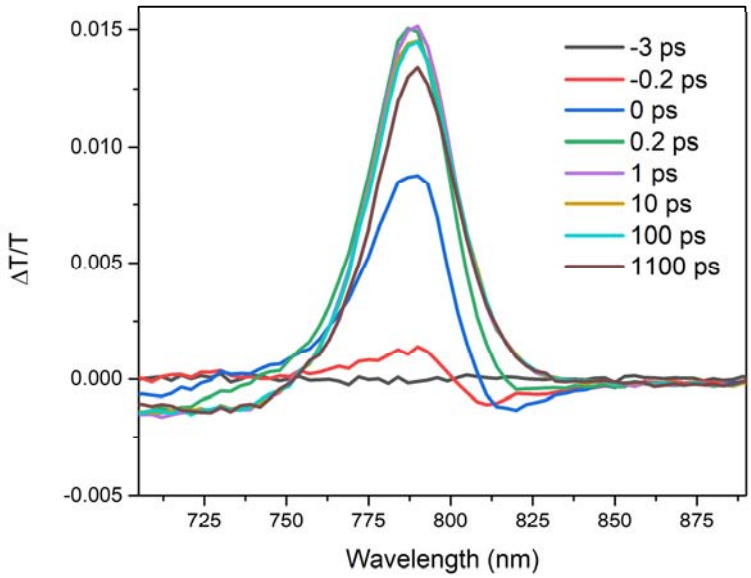

Figure S7. TA spectra with the pump wavelength at 690 nm. Ensemble of TA spectra

of $Cs_{0.1}FA_{0.9}PbI_3$ thin films at different delay times and change of transmission $\Delta T/T$ was plotted. Pump energy is 50 nJ per pulse with dia. 3.5 mm of light spot at the wavelength of 690 nm and the probe wavelength at 790 nm.

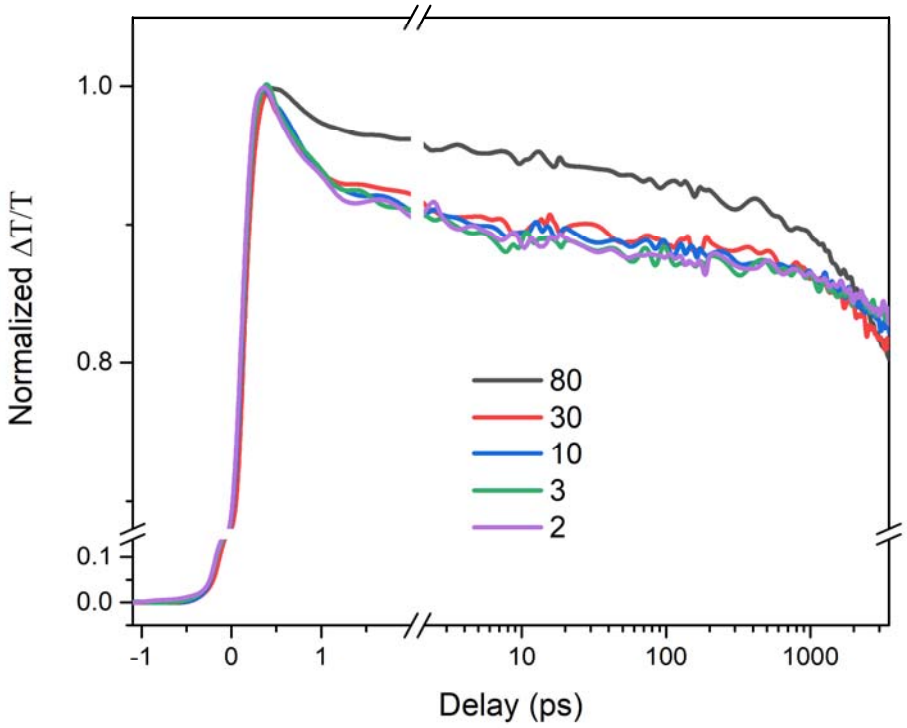

Figure S8. Pump intensity-dependent TA dynamics with the pump wavelength at 690 nm and the probe at 790 nm. The normalized changes of transmission $\Delta T/T$ were plotted corresponding to different pump energy from 80 to 2 nJ per pulse.

7. Fitting results

To quantitatively study the photogenerated carrier dynamics in the linear response range, the curve was fitted by triple exponential decay convoluted by the time resolution function as

$$f(t) = IRF \otimes \left(A_1 e^{-\frac{t-t_0}{t_1}} + A_2 e^{-\frac{t-t_0}{t_2}} + A_3 e^{-\frac{t-t_0}{t_3}} \right) + c \qquad \text{(S2)}$$

where A_1, A_2 and A_3 are the initial quantities of three decays, t_1, t_2 and t_3 are their

lifetimes, t_0 is the time zero, and IRF is the response function of TA system, which can be described as

$$IRF = A_0 e^{-\frac{(t-t_0)^2}{2\sigma^2}} \quad \text{(S3)}$$

And the time resolution is $2\sqrt{2ln2} \times \sigma \approx 2.355\sigma$, about 325 fs. t_3 is much larger than the delay line range, so the formula can be approximate to

$$f(t) \approx IRF \otimes \left(A_1 e^{-\frac{t-t_0}{t_1}} + A_2 e^{-\frac{t-t_0}{t_2}} + A_3 (1 - \frac{t-t_0}{t_3}) \right) + c \quad \text{(S4)}$$

8. Estimation of the Shockley-Queisser limit including the trapping effect

The utilization percentage of photogenerated carriers at the wavelength of λ is given by

$$\eta(\lambda) = \frac{A_3}{A_1 + A_2 + A_3} \quad \text{(S5)}$$

For 515 nm, the percentage of free carriers is 65.3%. For 690 nm, it is 83.7%.

Assume that the proportion of surface carrier density generated by 690 nm is x, and the bulk carrier is $(1 - x)$. The trapping factor of surface carriers is φ_s, and that of bulk carriers is φ_b. The transmission depth at 690 nm is 3.614 times of that at 515 nm, so the surface carrier density generated by 515 nm pump is assumed 3.614 times of that by 690 nm. Then from the equation

$$x\varphi_s + (1 - x)\varphi_b = 1 - 0.837 = 0.163 \quad \text{(S6)}$$

$$3.614x\varphi_s + (1 - 3.614x)\varphi_b = 1 - 0.653 = 0.347 \quad \text{(S7)}$$

we can obtain $\varphi_b = 0.0926$. It was reported that surface trap density is more than 10-100 times higher than that of bulk.[2] We assume that all the surface carriers can be trapped, that is $\varphi_s = 1$, and hence $x = 0.0776$.

We estimated the Shockley-Queisser limit including the trapping effect based on the detailed balance limit as below.[3, 4] At steady state the external current density J_{ext} in

a solar cell is given by

$$J_{ext} = J_{max} - J_r(V) \tag{S8}$$

where J_{max} is the current density corresponding to the total generation of electron hole pairs by incident sunlight, and J_r(V) is the radiative recombination current density at an external applied voltage, V. J_r(V) was calculated according to

$$J_r(E_g, V) = f_g q \int_{E_g}^{\infty} \frac{2\pi E^2}{h^3 c^2 \left(e^{\frac{E-qV}{kT}} - 1\right)} dE \tag{S9}$$

where E_g is the band gap energy, f_g is a geometrical factor, equal to 2 assuming that the solar cell emits radiation from both the front and rear sides, q is the elementary charge, h is the Planck constant, c is the vacuum speed of light, k is the Boltzmann constant, and T is the solar cell temperature. The maximum power point voltage was calculated according to

$$V_{mpp} = \max(V \cdot J_{ext}) \tag{S10}$$

and the J_{mpp} was calculated according to

$$J_{mpp} = J_{max} - J_r(V_{mpp}) \tag{S11}$$

The band gap is 790 nm, that is E_g is 1.569 V. We calculated that V_{mpp} equaled to 1.181 V, J_{mpp} was 260 A/m^2, and the Shockley-Queisser limit was 30.7%.

Concerning the Shockley-Queisser limit including the trapping effect, the carrier trapping can decrease the short circuit current. The external current density J_{ext} in Equation (S7) was rewritten as

$$J_{ext} = \int_0^{\lambda_g} j(\lambda) \cdot \eta(\lambda) d\lambda - J_r(V) \tag{S12}$$

where $j(\lambda)$ is the spectral current density, and λ_g is the band gap wavelength. We calculated that V_{mpp} equaled to 1.173 V, J_{mpp} was 191.9 A/m^2. The Shockley-Queisser limit including the trapping effect was obtained as 22.5%.

9. TA dynamics of the $PbCl_2$ doped $Cs_{0.1}FA_{0.9}PbI_3$ thin film

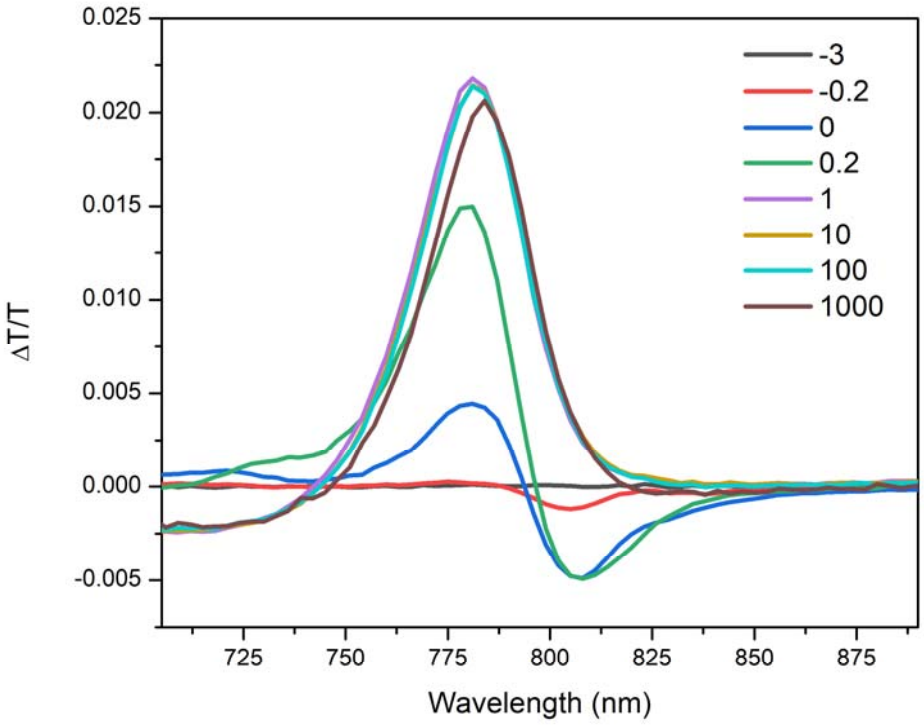

Figure S9. TA Spectra of $PbCl_2$ doped thin film. Ensemble of TA spectra of 5% $PbCl_2$ doped $Cs_{0.1}FA_{0.9}PbI_3$ thin films at different delay times and change of transmission $\Delta T/T$ was plotted. Pump energy is 50 nJ per pulse at the wavelength of 515 nm.

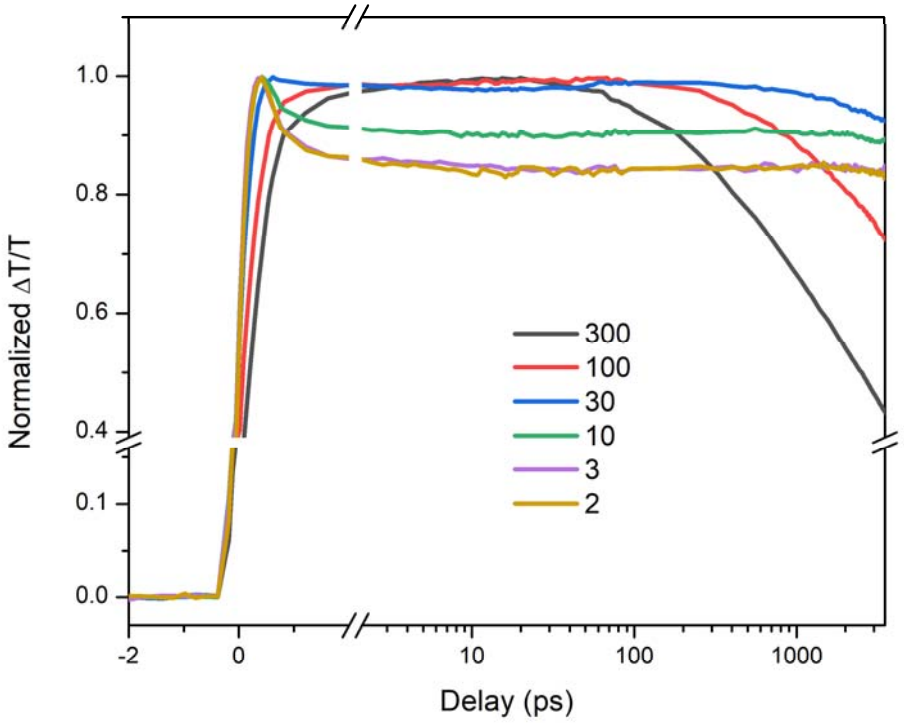

Figure S10. Pump intensity-dependent TA dynamics of $PbCl_2$ doped thin film. TA curves of 5% $PbCl_2$ doped $Cs_{0.1}FA_{0.9}PbI_3$ thin film with the pump wavelength at 515 nm and the probe at 784 nm. The normalized changes of transmission $\Delta T/T$ were plotted corresponding to different pump energy from 300 to 2 nJ per pulse.

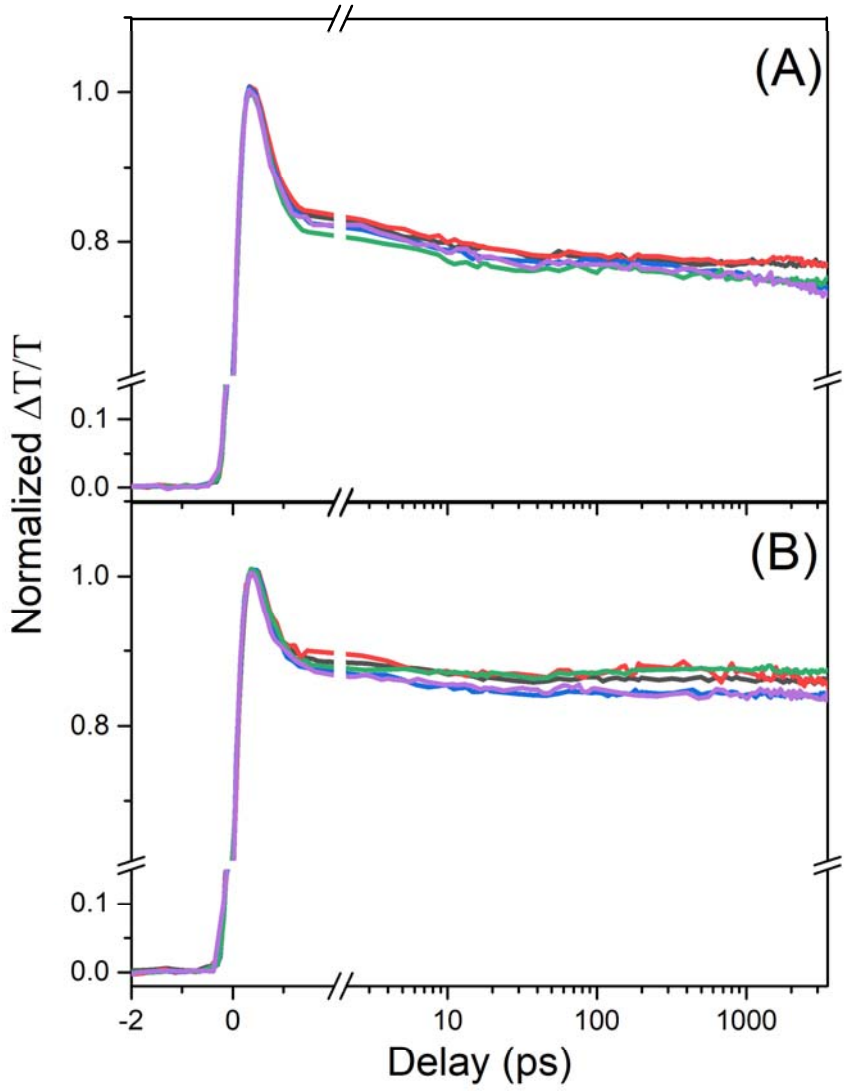

Figure S11. $PbCl_2$ passivation effect. Comparison of carrier dynamics of 5 pristine (A) and 5 $PbCl_2$ doped (B) $Cs_{0.1}FA_{0.9}PbI_3$ perovskite thin film samples by measuring the TA curves with pump energy of 3 nJ at 515 nm and probe at 790 nm and 784 nm, respectively, in the linear response range.

Table S1. Fitting results of TA curve in Figure S13 by using Equation S4.

pristine	1#	2#	3#	4#	5#
A_1	0.318±0.013	0.306±0.013	0.339±0.014	0.370±0.016	0.355±0.015
t_1 (ps)	0.68±0.05	0.64±0.05	0.60±0.05	0.58±0.05	0.53±0.04
A_2	0.033±0.005	0.039±0.007	0.039±0.007	0.037±0.008	0.047±0.005
t_2 (ps)	29±11	18.1±5.7	14.5±4.5	13.9±4.7	14.7 ±2.6
A_3	0.766±0.003	0.762±0.002	0.759±0.002	0.759±0.002	0.755±0.002
t_3 (ps)	$40\pm16\times10^4$	$27.5\pm7.0\times10^4$	$74.9\pm4.9\times10^3$	$17\pm2.7\times10^4$	$74.0\pm4.0\times10^3$
η	68.6%	68.8%	66.8%	65.1%	65.2%

$PbCl_2$ doped	1#	2#	3#	4#	5#
A_1	0.253±0.012	0.224±0.012	0.244 ± 0.013	0.225 ± 0.011	0.265±0.013
t_1 (ps)	0.65±0.07	0.62±0.07	0.63±0.07	0.64±0.04	0.54±0.04
A_2	0.039±0.007	0.014±0.007	0.017 ± 0.007	0.000 ± 0.020	0.018±0.004
t_2 (ps)	17.5±5.6	$1.3\pm1.1\times10^1$	12.0±8.1	$2.2 \pm 1.8 \times 10^2$	11.4±4.0
A_3	0.808±0.003	0.857±0.002	0.836 ± 0.002	0.868 ± 0.003	0.849±0.002
t_3 (ps)	$> 1.0\times10^6$	$> 1.0\times10^6$	$5.3 \pm 2.0 \times 10^5$	$6.7 \pm 5.0 \times 10^5$	$24.3 \pm 3.3 \times 10^4$
η	73.4%	78.3%	76.2%	79.4%	75.0%

References

1. Li, H., Hu, G., Li, B.-H., Zeng, W., Zhang, J., Wang, X.*, et al.* Ultrahigh sensitive transient absorption spectrometer. *Rev. Sci. Instrum.* 2021, **92**(5)**:** 053002.

2. Ni, Z., Bao, C., Liu, Y., Jiang, Q., Wu, W.-Q., Chen, S.*, et al.* Resolving spatial and energetic distributions of trap states in metal halide perovskite solar cells. *Science* 2020, **367**(6484)**:** 1352-1358.

3. Shockley, W., Queisser, H.J. Detailed balance limit of efficiency of p-n junction solar cells. *J. Appl. Phys.* 1961, **32**(3)**:** 510-519.

4. Rühle, S. Tabulated values of the Shockley–Queisser limit for single junction solar cells. *Sol. Energy* 2016, **130:** 139-147.